Cell-to-cell variability in organelle abundance reveals mechanisms of organelle biogenesis

Sandeep Choubey,[1,*] Dipjyoti Das,[2] and Saptarshi Majumdar[1]
[1]*Max Planck Institute for the Physics of Complex Systems, Nöthnitzerstraße 38, 01187 Dresden, Germany*
[2]*Department of Molecular, Cellular and Developmental Biology, Yale University, New Haven, Connecticut 06511, USA*

(Received 7 February 2019; published 6 August 2019)

How cells regulate the number of organelles is a fundamental question in cell biology. While decades of experimental work have uncovered four fundamental processes that regulate organelle biogenesis, namely, *de novo* synthesis, fission, fusion, and decay, a comprehensive understanding of how these processes together control organelle abundance remains elusive. Recent fluorescence microscopy experiments allow for the counting of organelles at the single-cell level. These measurements provide information about the cell-to-cell variability in organelle abundance in addition to the mean level. Motivated by such measurements, we build upon a recent study and analyze a general stochastic model of organelle biogenesis. We compute the exact analytical expressions for the probability distribution of organelle numbers, their mean, and variance across a population of single cells. It is shown that different mechanisms of organelle biogenesis lead to distinct signatures in the distribution of organelle numbers which allow us to discriminate between these various mechanisms. By comparing our theory against published data for peroxisome abundance measurements in yeast, we show that a widely believed model of peroxisome biogenesis that involves *de novo* synthesis, fission, and decay is inadequate in explaining the data. Also, our theory predicts bimodality in certain limits of the model. Overall, the framework developed here can be harnessed to gain mechanistic insights into the process of organelle biogenesis.

DOI: 10.1103/PhysRevE.100.022405

I. INTRODUCTION

An organelle is a spatial compartment in eukaryotic cells [1,2] that performs a specialized function. Examples of organelles include vacuoles, Golgi bodies, endoplasmic reticulum, etc. Cells tightly regulate organelle number in response to environmental and intracellular cues [1–3]. For instance, the number of mitochondria in mammals is tightly regulated in response to their metabolic needs [4]. Yeast cells significantly downregulate vacuole abundance during starvation, or upon hypotonic shock [5]. These instances raise the natural question: how is organelle abundance regulated in cells?

Fluorescence microscopy studies of live and fixed cells over the years have led to the discovery of four basic processes that control organelle numbers in cells, namely, *de novo* synthesis from a preexisting membrane source [6,7], fission [8–11], fusion [5,12–18], and decay through autophagy or random partitioning during cell division [2,19–21]. For example, mitochondria regulation involves fission and fusion [22]. An important property of organelle biogenesis is that all of the aforementioned processes are inherently stochastic [23,24]. This has led to an alternative approach to unraveling the mechanisms of biogenesis in cells by counting organelle numbers [2,23,25]. Then, the measured steady-state distribution of organelles across a cell population can be used to infer the dynamics of their biogenesis. In a recent study, Mukherji *et al.* [23] put forward a general and elegant model of organelle biogenesis consisting of these processes. Using a combination of theory and experiments the authors exploited the cell-to-cell variability in organelle abundance to uncover the kinetic rules of organelle biogenesis. This approach led to newer insights, such as that Golgi body abundance is controlled through the balance of de novo synthesis and decay [23]. While this study along with another follow up work [25] represent the first attempts to uncover the mechanisms of organelle biogenesis using cell-to-cell variability or noise in organelle abundance, these aforementioned studies only looked into the specific limits of the general model. A comprehensive understanding of the impact of different mechanisms underlying organelle biogenesis on the cell-to-cell variability in organelle abundance remains in its infancy.

The goal of this manuscript is to carry out such a systematic exploration. First, we compute the exact analytical expressions for the probability distribution, mean, and variance of the organelle distribution for the general model, and all the different limits of this model. We demonstrate the utility of our theoretical results by applying them to published datasets for peroxisome counts at the single cell level. We show that a proposed mechanism of biogenesis [23,25], where peroxisome number is controlled through de novo synthesis, fission, and decay is inadequate in explaining the data. Moreover, we discover that in a region of parameter space the model predicts bimodality in organelle abundance. Overall, our study provides a general and comprehensive analysis of how different mechanisms of organelle biogenesis control organelle number *in vivo*, and illustrates a recipe to extract mechanistic insights from single cell organelle measurements.

*sandeep@pks.mpg.de

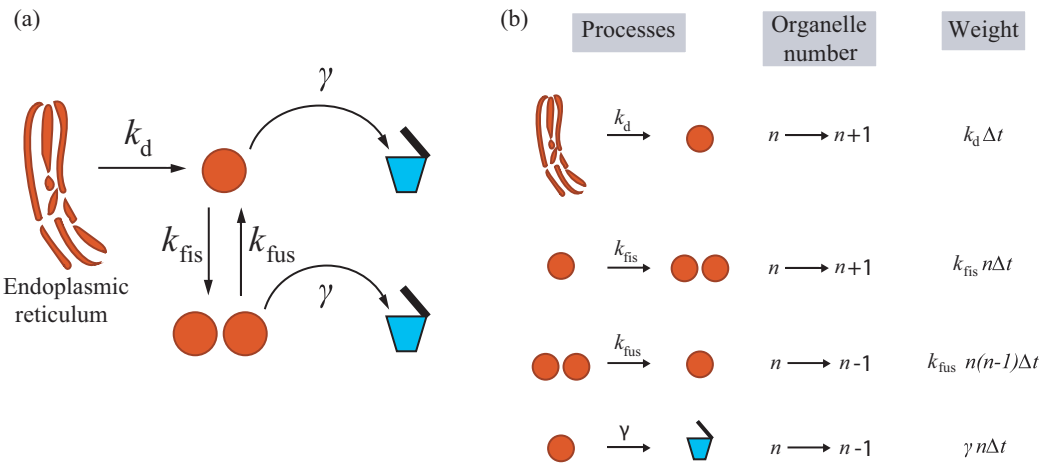

FIG. 1. Model of organelle biogenesis. (a) Organelle biogenesis involves four mechanisms, namely, *de novo* synthesis, fission, fusion, and decay. The probability per unit time of *de novo* synthesis is given by zeroth-order rate constant k_d. $k_{\rm fis}$ is the first-order rate constant characterizing fission, $k_{\rm fus}$ is the second-order rate constant defining fusion, and γ is the first-order rate constant defining decay, as proposed by Mukherji and O'Shea [23]. From this model, we compute the probability distribution of organelle abundance as well as its mean and variance. (b) List of possible reactions leading to either an increase or decrease in the organelle number and their respective weights. The weights constitute the probability that each reaction will occur during a time interval, Δt.

II. MODEL

To shed light on how the mechanisms of organelle biogenesis impact the cell-to-cell variability in organelle abundance across a cell line, we build upon a recent study by Mukherji and O'Shea [23,25]. In this study, the authors proposed a general model of organelle biogenesis involving four different processes: *de novo* synthesis, fission, fusion, and decay, as shown in Fig. 1(a). This phenomenological model essentially combines the hitherto observed mechanisms of biogenesis of various organelles such as mitochondria, vacuole, peroxisome, Golgi body, etc. [6,16]. As shown in Fig. 1(a), in this model, *de novo* synthesis of an organelle happens with a zeroth-order rate constant k_d. Through fission one organelle copy divides and produces two copies at first-order rate constant $k_{\rm fis}$ per organelle. Two organelle copies fuse at second-order rate constant $k_{\rm fus}$ per organelle squared, and form one organelle copy. Finally, an organelle copy can decay with a first-order rate constant γ per organelle. It is evident from the model that *de novo* synthesis and fission increase the number of organelles, while fusion and decay decrease their number [see Fig. 1(b)]. Through an interplay between these opposing processes, the organelle abundance reaches a steady state, whereby the distribution of number of organelles does not change in time. While attaining the steady state in the different limits of the model is not always guaranteed (for details, see Materials and Methods), such an assumption has been useful and reasonable in explaining the experimental data [23,25]. In this regime, one can analyze the different limits of the general model and make specific predictions about the steady-state organelle abundance.

For the investigation of the steady-state properties of the model, it is instructive to delineate the above processes [23,25] in the space of organelle number, as shown in Fig. 1(b). These processes and their corresponding weights allow us to employ a stochastic framework and monitor the time evolution of the organelle number. The probability distribution $P(n, t)$ of having n organelles in a cell at a time t is given by the master equation [23]

$$\begin{aligned}\frac{dP(n,t)}{dt} &= [k_d + k_{\rm fis}(n-1)]P(n-1,t) \\ &\quad + [\gamma + k_{\rm fus}n](n+1)P(n+1,t) \\ &\quad - [k_d + k_{\rm fis}n + \gamma n + k_{\rm fus}n(n-1)]P(n,t). \qquad (1)\end{aligned}$$

The above equation is an agglomeration of all possible steps that lead to either an increase or decrease in organelle copy number [see the processes in Fig. 1(b)]. In principle, the master equation contains all the information about the organelle number distribution and its moments such as the mean and variance, etc. However, obtaining exact solutions for the moments and the distribution from this master equation is challenging [23,25]. Alternatively, we make use of the detailed balance condition [25,26] to obtain the steady-state organelle number distribution (see Materials and Methods). From these steady-state distributions, we compute the mean and variance of organelle numbers using standard functions in MATHEMATICA.

III. DIFFERENT MECHANISMS OF ORGANELLE BIOGENESIS PROVIDE DISTINCT "FINGERPRINTS" IN CELL-TO-CELL VARIABILITY IN ORGANELLE ABUNDANCE

To expound the effect of different mechanisms of organelle biogenesis on the cell-to-cell variability in organelle abundance, we consider different possible limits of the general model. For instance, consider a model of biogenesis that involves nonzero rates of *de novo* synthesis and decay, while contributions from fission and fusion processes are vanishing; we call this model *de novo* synthesis decay. We identify six such limits of the general model that reach the steady state: (i) *de novo* synthesis-decay, (ii) fission-fusion, (iii) *de novo* synthesis-fusion, (iv) *de novo* synthesis-fission-decay,

TABLE I. Formulas for the steady-state probability distributions, as well as for their means and Fano factors for different models of organelle biogenesis, are shown. We discuss each of the seven models in the first results section. The different special functions that arise in these different formulas are defined as follows: ${}_nF_m(a_1, a_2, ..., a_n; b_1, b_2, ...b_m; z)$ is the generalized hypergeometric function that has n parameters of type 1 and m parameters of type 2. ${}_nF_m^R(a_1, a_2, ..., a_n; b_1, b_2, ...b_m; z) \equiv \frac{{}_nF_m(a_1,a_2,...,a_n;b_1,b_2,...b_m;z)}{\Gamma(b_1)\Gamma(b)..\Gamma(b_m)}$ is known as the regularized hypergeometric function, where $\Gamma(x)$ is the gamma function. Moreover, $I_n(x)$ is the modified Bessel function of the first kind of order n, where n is an integer. For a detailed discussion of special functions please see the Refs. [33,34].

Mechanism	Steady-state probability distribution	Mean	Fano factor
De novo-decay	$\frac{1}{n!}\lambda^n e^{-\lambda}$, where $\lambda = k_d/\gamma$.	λ	1
Fission-fusion	$\frac{1}{n!}\phi^n\left(\frac{e^{-\phi}}{1-e^{-\phi}}\right)$, where $\phi = k_{fis}/k_{fus}$. *for* $n = 1,2,3....$ $= 0$, *for* $n = 0$	$\frac{\phi e^{\phi}}{(e^{\phi}-1)}$	$1-\frac{\phi}{(e^{\phi}-1)}$
De novo-fusion	$\frac{1}{n!(n-1)!}\beta^{n-1/2}\frac{1}{I_1\left(2\sqrt{\beta}\right)}$, *for* $n = 1,2,3....$ $= 0$, *for* $n = 0$ where $\beta = k_d/k_{fus}$.	$\sqrt{\beta}\frac{I_0\left(2\sqrt{\beta}\right)}{I_1\left(2\sqrt{\beta}\right)}$	$1-\frac{{}_0F_1^R(1,\beta)}{{}_0F_1^R(2,\beta)}+\frac{\beta\,{}_0F_1^R(2,\beta)}{{}_0F_1^R(1,\beta)}$
De novo-fission - fusion	$\frac{1}{\alpha}\frac{\phi^{n-1}}{n!(n-1)!}\frac{\Gamma(\alpha+n)}{\Gamma(\alpha)}\frac{1}{{}_1F_1(1+\alpha,2,\phi)}$, *for* $n = 1,2,3....$ $= 0$, *for* $n = 0$ where $\alpha = k_d/k_{fis}$, $\phi = k_{fis}/k_{fus}$.	$\frac{{}_1F_1(1+\alpha,1,\phi)}{{}_1F_1(1+\alpha,2,\phi)}$	$\frac{{}_2F_2(\{2,1+\alpha\},\{1,1\},\phi)}{{}_1F_1(1+\alpha,1,\phi)}-\frac{{}_1F_1(1+\alpha,1,\phi)}{{}_1F_1(1+\alpha,2,\phi)}$
De novo-fission - decay	$\frac{q^n(1-q)^{\alpha}}{n!}\frac{\Gamma(\alpha+n)}{\Gamma(\alpha)}$, where $\alpha = k_d/k_{fis}$, $q = k_{fis}/\gamma$.	$\frac{q\alpha}{(1-q)}$	$\frac{1}{(1-q)}$
De novo-fusion - decay	$\frac{\beta^n}{n!}\frac{\Gamma(\delta)}{\Gamma(\delta+n)}\frac{1}{{}_0F_1(\delta,\beta)}$, where $\beta = k_d/k_{fus}$, $\delta = \gamma/k_{fus}$.	$\frac{\beta\,{}_0F_1^R(1+\delta,\beta)}{{}_0F_1^R(\delta,\beta)}$	$1-\frac{\beta\,{}_0F_1^R(1+\delta,\beta)}{{}_0F_1^R(\delta,\beta)}+\frac{\beta\,{}_0F_1^R(2+\delta,\beta)}{{}_0F_1^R(1+\delta,\beta)}$
De novo-fission - fusion-decay	$\frac{\phi^n}{n!}\frac{\Gamma(\alpha+n)}{\Gamma(\alpha)}\frac{\Gamma(\delta)}{\Gamma(\delta+n)}\frac{1}{{}_1F_1(\alpha,\delta,\phi)}$ where $\alpha = k_d/k_{fis}, \delta = \gamma/k_{fus}, \phi = k_{fis}/k_{fus}$.	$\frac{\alpha\phi}{\delta}\frac{{}_1F_1(1+\alpha,1+\delta,\phi)}{{}_1F_1(\alpha,\delta,\phi)}$	$1-\frac{\alpha\phi\,{}_1F_1^R(1+\alpha,1+\delta,\phi)}{{}_1F_1^R(\alpha,\delta,\phi)}+\frac{(1+\alpha)\phi\,{}_1F_1^R(2+\alpha,2+\delta,\phi)}{{}_1F_1^R(1+\alpha,1+\delta,\phi)}$

(v) *de novo* synthesis-fusion-decay, and (vi) *de novo* synthesis-fission-fusion. For a detailed discussion on the conditions of reaching the steady state for the different possible mechanisms, see Materials and Methods. Although the (iii) *de novo* synthesis-fusion and (vi) *de novo* synthesis-fission-fusion models do have steady states in terms of organelle number, because of the presence of the de novo synthesis process the organelle size will keep increasing. Hence, these models can be biologically relevant only if there are other cellular mechanisms [21] to maintain mass balance without altering the organelle number (see Materials and Methods for a discussion). It must be noted that we consider only those models which show stationarity in the strict mathematical sense. Clearly, one cannot rule out the possibility of fission-decay or fission-fusion-decay model being biologically relevant, if the fission rate is much greater than the decay rate (for a detailed discussion, see Materials and Methods). We compute the exact steady-state distribution of organelle numbers, its mean, and variance for each of these six cases as well as the general model (see Table I). With these results at hand, we perform a comparative analysis of how these different mechanisms affect the cell-to-cell variability in organelle abundance. To carry out such an analysis, throughout the rest of the paper we quantify the cell-to-cell variability using a statistical quantity, known as the Fano factor [23,27], which is defined as the ratio of the variance and the mean. We describe the behavior of the Fano factor as a function of the mean as we change the various experimentally tunable rates associated with the four processes.

A. *De novo* synthesis-decay

The *de novo* synthesis-decay model is a good starting point owing to its simplicity [23,25]. Abundance of many organelles such as Golgi body [23,28–31] is controlled through this mechanism [6,19,28,32]. The number distribution of organelles for this model is characterized by the Poisson distribution (shown in Table I) [23], which is defined by one effective parameter, given by the ratio of *de novo* synthesis and decay rate constants. One of the key properties of a Poisson distribution is that its mean and variance are equal, i.e., the Fano factor for this model is 1, independent of the values of *de*

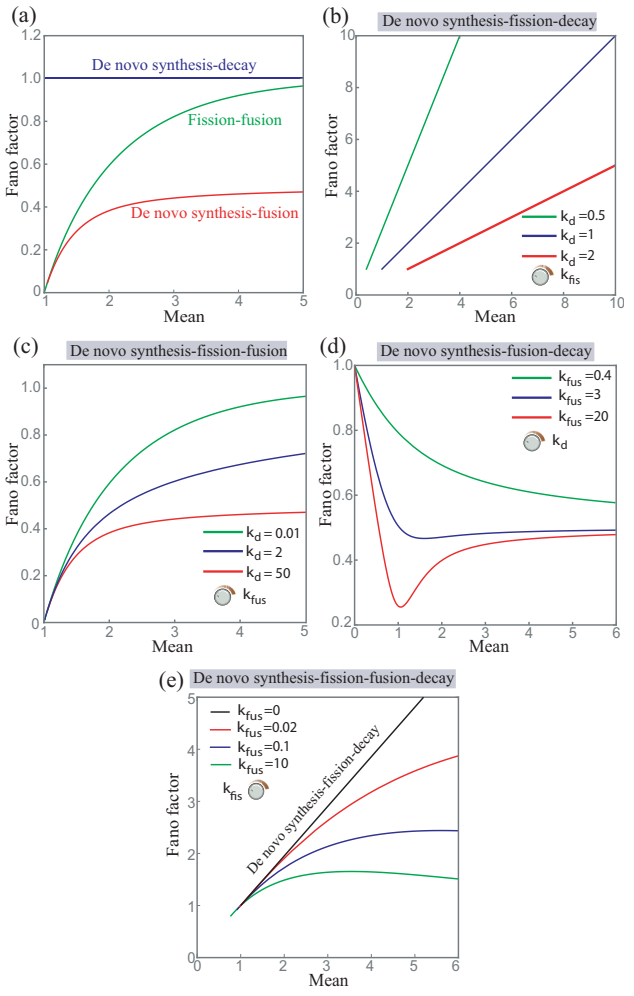

FIG. 2. Noise profiles for different models of organelle biogenesis. Using the detailed balance condition [25,26], we computed the Fano factor of the organelle number distribution for the different models of organelle biogenesis. (a) Three different models of biogenesis involving two processes: *de novo* synthesis-fusion (red), fission-fusion (green), and *de novo* synthesis-decay (blue). These models lead to qualitatively distinct predictions for the Fano factor as a function of the mean. (b) *De novo* synthesis-fission-decay: We tune the fission rate constant while keeping the other rates fixed to generate the plots. The family of curves corresponds to the different values of k_d, where we keep the other rates fixed, $\gamma = 1\,t^{-1}$. (c) *De novo* synthesis-fission-fusion: Rate of fission is tuned to generate the plots, while we keep the other rate constants fixed. The family of curves corresponds to the different values of k_d; fusion rate is given by $k_{\rm fus} = 1\,t^{-1}$. (d) *De novo* synthesis-fusion-decay: The *de novo* synthesis rate is tuned to make the Fano factor versus mean plots. The family of curves corresponds to the different values of $k_{\rm fus}$. The decay rate is given by $\gamma = 1\,t^{-1}$. (e) In this plot, we vary $k_{\rm fis}$, while keeping k_d and γ constant (value of both the rate constants have been kept as 1) and explore how the noise profile evolves over different values of $k_{\rm fus}$. When $k_{\rm fus} = 0$, the curve becomes a straight line which is characteristic for the *de novo* synthesis-fission-decay.

novo synthesis and decay rate constants, as shown in Fig. 2(a). This model thus serves as a good reference point for the comparison of different models, wherein a deviation of the Fano factor from 1 indicates the presence of other processes. This feature holds the key to our analysis in the rest of the paper.

B. *De novo* synthesis-fusion

The *de novo* synthesis-fusion model is fully characterized by one effective parameter, defined by the ratio of the rate constants characterizing *de novo* synthesis and fusion. For this model the steady-state number of organelles never goes to zero. The Fano factor increases as a function of the mean and asymptotically goes to 0.5 when we alter one of the rate constants of this model while keeping the other one fixed, as shown in Fig. 2(a). While *de novo* synthesis happens at a constant rate, fusion depends on the square of the number of organelles. Such a reduction in the overall noise level can be comprehended by comparing the *de novo* synthesis-decay and *de novo* synthesis-fusion models. These two models differ from each other owing to the manner in which the number of organelles decreases; the reduction in organelle number happens through two different processes, namely decay and fusion. While decay goes linearly with organelle number, fusion depends on the square of the organelle number, as shown in Fig. 1(b). The relatively rapid change in the "weight" (or, equivalently, in the rate) of fusion as the organelle number fluctuates around its mean value has a strong restoring tendency, thus making the distribution narrower compared to decay. Consequently, the Fano factor becomes less than 1. The impact of fusion on noise in organelle numbers has been reported before by Mukherji and O'Shea [23].

C. Fission-fusion

Next, we consider the fission-fusion model. In yeast and mammalian cells, the biogenesis of organelles such as vacuole and mitochondria involves both fission and fusion [15,22,35–37]. For the fission-fusion model, we find that the organelle abundance is given by a truncated Poisson distribution, fully characterized by the ratio of the rate constants characterizing fission and fusion. This result is in agreement with a previous theoretical study [25]. It is evident that for this model the number of organelles can never go below 1. As shown in Fig. 2(a), when we tune either one of the two rates of the model while keeping the other rate fixed, the Fano factor increases as a function of the mean and asymptotically approaches 1. In other words, with an increasing mean, the organelle number distribution approaches the Poisson distribution, characteristic of the *de novo* synthesis-decay model [23,25].

Clearly, the three models corresponding to combinations of two processes lead to distinct predictions for the Fano factor as a function of the mean, as shown in Fig. 2(a). Since each of these three models depends on one effective parameter, the Fano factor as a function of the mean for each of them is uniquely defined. The results obtained for these models serve as reference points for exploring the models consisting of combinations of three processes.

D. *De novo* synthesis-fission-decay

De novo synthesis-fission-decay model is defined by two effective parameters (ratio of the *de novo* synthesis and fission rate constants, and fission and decay rate constants, respectively; see Table I). We seek to explore the behavior of the Fano factor as a function of the mean for this model. This

can be achieved in three different ways: (i) change the *de novo* synthesis rate constant keeping the fission and decay rate constants fixed; (ii) change the fission rate constant keeping the *de novo* synthesis and decay rates constants fixed; and (iii) alter the decay rate constant keeping the fission and *de novo* synthesis rate constants fixed. Here we choose the second scenario, motivated by the fact that the fission rate constant of, for instance, peroxisome can be tuned by knocking down genes such as *DNM1*, *VPS1*, etc. The Fano factor versus mean plots for the other two scenarios are shown in the Supplemental Material, Fig. S1 [38]. Using the *de novo* synthesis-decay model as our reference, it is evident that the Fano factor increases monotonically as a function of the mean, as shown in Fig. 2(b). Clearly, the inclusion of the fission process enhances the overall noise, which is in agreement with previous studies [23,25].

E. *De novo* synthesis-fission-fusion

The *de novo* synthesis-fission-fusion model is defined fully by two effective parameters (ratio of the *de novo* synthesis and fission rate constant and fission and fusion rate constants), as shown in Table I. Like the previous model, we can expound the behavior of the cell-to-cell variability for this model by tuning one of the parameters while keeping the other two parameters constant. As an example, we alter the *de novo* synthesis rate constant keeping the fission and fusion rate constants fixed [see Fig. 2(c)]; the rest of the two scenarios are shown in the Supplemental Material, Fig. S2 [38]. Using the fission-fusion model as a reference, we find that as the *de novo* synthesis rate constant is increased, the *de novo* synthesis-fission-fusion model predicts an overall lowering of the noise level [see Fig. 2(b)]. Moreover, the Fano factor as a function of the mean approaches the *de novo* synthesis-fusion model. On the other hand, when the fission rate constant is increased keeping the *de novo* synthesis rate constant fixed, the Fano factor increases as a function of the mean and approaches the curve defining the fission-fusion model. Indeed, the cell-to-cell variability in organelle abundance for this model is bound by the Fano factor-mean curves defining the fission-fusion and *de novo* synthesis-fusion model.

F. *De novo* synthesis-fusion-decay

The *de novo* synthesis-fusion-decay model is characterized by two effective parameters (ratio of the *de novo* synthesis and fusion rate constants, and fusion and decay rate constants, respectively; see Table I). Fano factor as a function of the mean is plotted by altering the *de novo* synthesis rate constant while keeping the fusion and decay rate constants fixed; see Fig. 2(d). For the other possible scenarios, see the Supplemental Material, Fig. S3 [38]. Using the *de novo* synthesis-fusion model as our reference, we find that the introduction of the decay rate enhances the noise level, as shown in Fig. 2(d). Moreover, the Fano factor shows a nonmonotonic behavior as a function of the mean as we alter the decay rate constant for when the fusion rate constant is much greater than the decay rate constant [see the red curve in Fig. 2(d)]. Initially, when the mean is less than 1, the Fano factor decreases and shows a minimum around a value of mean equal to 1. Subsequently, the Fano factor increases with the mean and asymptotically goes to 1. The reason for this nonmonotonic behavior is that the fusion process cannot occur when the organelle number is less than 2, and hence decay is dominant. On the other hand, at large organelle numbers, the fusion process dominates over the decay process since the fusion rate constant is much greater than the decay rate constant. As a result, the Fano factor of the organelle number switches from a Poissonian behavior (set by the *de novo* synthesis-decay process) to a behavior set by the *de novo* synthesis-fusion process [Fig. 2(d)]. This crossover produces the observed nonmonotonic behavior in the Fano factor. For the *de novo* synthesis-fusion-decay model, the upper bound of the noise level is set by the noise in a Poisson process, characteristic of the *de novo* synthesis-decay model, while the lower bound is set by the noise in the *de novo* synthesis-fusion process. It is evident that the presence of the fusion process decreases noise in organelle abundance which is consistent with previous studies [23,25].

G. *De novo* synthesis-fission-fusion-decay

Finally, we analyze the general model consisting of all the four processes and explore how these four processes in conjunction impact organelle abundance across a cell population. This model is characterized by three effective parameters (ratio of the *de novo* synthesis and fission rate constant, fission and fusion rate constant, and fusion and decay rate constant), as shown in Table I. Using the analytical expressions from Table I, we can study the behavior of the Fano factor as a function of the mean by altering one of the parameters of the model while keeping the others fixed. For instance, when we alter the fission rate constant (keeping the other rate constants fixed), the Fano factor shows a nonmonotonic behavior as a function of the mean, as shown in Fig. 2(e). For a small mean level, the Fano factor increases with the mean as we increase the fission rate, which is characteristic of the *de novo* synthesis-fission-decay model. For higher organelle copy numbers the fission and fusion processes dominate [due to the weights of these processes, see Fig. 1(b)] and the Fano factor asymptotically approaches 1, after showing a peak in between. However, as the fusion rate tends to zero, the Fano factor manifests a linear behavior as a function of the mean abundance, characteristic of the *de novo* synthesis-fission-decay model. For a thorough analysis of the *de novo* synthesis-fission-fusion-decay model, see the Supplemental Material (Fig. S4) [38].

Overall, these results imply that we can discern between different mechanisms of organelle biogenesis based on the specific predictions they make for the Fano factor as a function of the mean.

IV. THE *DE NOVO* SYNTHESIS-FISSION-DECAY MODEL FAILS TO EXPLAIN THE NOISE IN PEROXISOME ABUNDANCE IN YEAST

To illustrate the usefulness of our theoretical results, we reanalyze previously published data for single-cell peroxisome counts in *Saccharomyces cerevisiae* [39]. In *Saccharomyces cerevisiae*, peroxisomes are primarily involved in

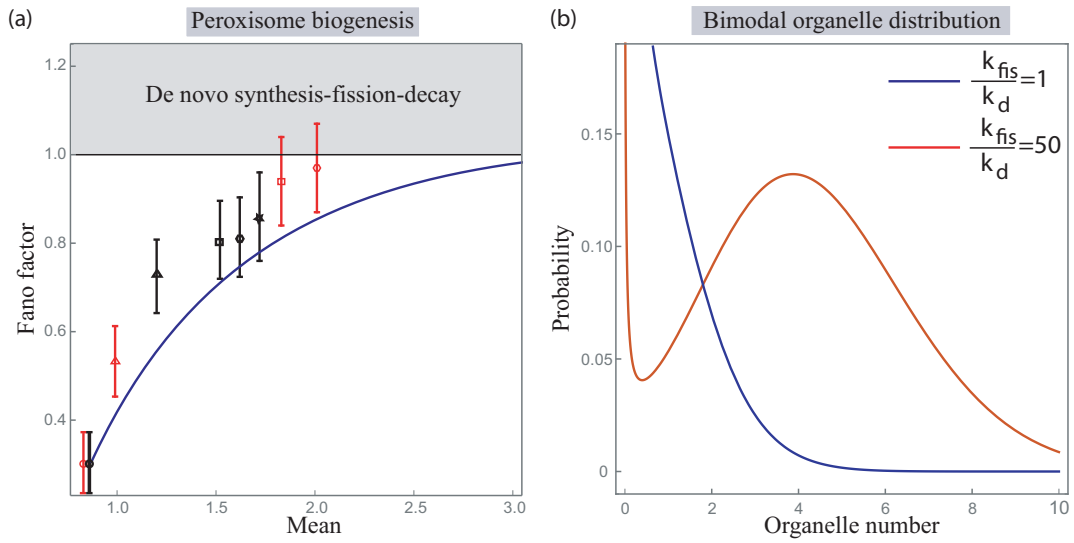

FIG. 3. (a) Peroxisome biogenesis. The black data points represent the experimentally measured Fano factor of peroxisome number distribution as a function of the mean for various *Saccharomyces cerevisiae* mutant strains, grown in glucose medium, with combinations of deleted *VPS1* and *DNM1*, taken from Ref. [39]. The data points represent the following mutants: (i) o vps1Δ*dnm1*Δ, (ii) Δ vps1Δ, (iii) □ *fis*Δ, (iv) ◊ WT, (v) ∗ *dnm1*Δ. The red data points represent the same yeast strains, grown in the oleic acid medium. Corresponding data points are given by (i) o vps1Δ*dnm1*Δ, (ii) Δ vps1Δ, (iii) □ *fis*Δ, (iv) ◊ *dnm1*Δ. The blue curve shows the *de novo* synthesis-fission-fusion-decay model prediction for how the Fano factor changes as a function of the mean when we alter the fission rate constant while keeping the other rate constants fixed. The other rate constants are given by $k_{\rm fus} = 34.3\,t^{-1}$, $k_d = 3.45\,t^{-1}$, and $\gamma = 1\,t^{-1}$. (B) Bimodality in organelle abundance: The steady-state number distributions of organelles are shown for different values of the *de novo* synthesis rate constant for the *de novo* synthesis-fission-fusion-decay model. When the rate of *de novo* synthesis is much greater than the fission rate, the organelle distribution manifests bimodality. The rate constants corresponding to the blue curve are $k_d = 0.1\,t^{-1}$,$k_{\rm fis} = 0.1\,t^{-1}$, $k_{\rm fus} = 1\,t^{-1}$, and $\gamma = 1\,t^{-1}$. The rate constants corresponding to the red curve are $k_d = 0.1\,t^{-1}$,$k_{\rm fis} = 5\,t^{-1}$, $k_{\rm fus} = 1\,t^{-1}$, and $\gamma = 1\,t^{-1}$.

the metabolism of various carbon and nitrogen sources, such as oleic acid, and purines, etc. The underlying mechanisms of peroxisome biogenesis remain elusive [40,41]. Various experimental studies have reported the role of *de novo* synthesis [6,42,43], fission [44,45] and decay [46] in controlling peroxisome number. Most recent studies [23,25] have systematically constructed a model (*de novo* synthesis-fission-decay) based on these experimental observations and showed that this model captures the essential features of the peroxisome distribution data in glucose and oleic acid-grown yeast cells.

Using our theoretical results, we put this model to the test by applying it to single-cell peroxisome abundance measurements [39]. This study by Kuravi *et al.* [39] seeks to unravel the role of the dynamin-related proteins such as Vps1, Dnm1, etc., in regulating the number of peroxisomes in *Saccharomyces cerevisiae*. The authors deleted various combinations of the genes, *VPS1*, and *DNM1* and noted the change in peroxisome count in glucose and oleic acid media. Interestingly, most of the mutants from this study [39] manifest a Fano factor of less than 1 [see Fig. 3(a)]. As shown before [see Fig. 2(c) and the Supplemental Material [38]), if the *de novo* synthesis-fission-decay model governs the biogenesis of an organelle, its Fano factor always remains equal to or greater than 1 [see Fig. 3(a)]. Hence, the *de novo* synthesis-fission-decay model of peroxisome biogenesis is inadequate. Our theoretical exploration showed [see Fig. 2(a)] that the Fano factor of organelle number distribution can go below 1 only if its biogenesis involves fusion. Motivated by this observation, we consider the *de novo* synthesis-fission-fusion-decay model consisting of all the four processes. To test this model, first we fit the peroxisome data for the dnm1-vps1 double-deletion yeast strain with the model to find the values of the individual rate constants (see Materials and Methods and Supplemental Material, Fig. S5 [38]). For simplification, we assume that the fission rate for this strain is vanishing since two of the key fission factors are not present in the cells. Hence, the *de novo* synthesis-fission-fusion-decay model reduces to the *de novo* synthesis-fusion-decay model, which is defined by two effective parameters. Having obtained the corresponding parameter values, we are in a position to test the *de novo* synthesis-fission-fusion-decay model by comparing the predictions this model makes against the data (for details see Materials and Methods). To achieve this goal, we plot the Fano factor as a function of the mean [Fig. 3(a)] as the fission rate is increased; it is assumed here that the fission rate would be higher for the wild type (WT) strain as well as the single-deletion strains that consist one of the three genes *DNM1*, *VPS1*, and *FIS1*. Next, we compare these predictions with the peroxisome abundance measurements in yeast cells grown in the glucose and oleic acid medium. The theory predictions match well with the data for yeast cells grown in the glucose medium. Interestingly, even for cells grown in the oleic acid medium, which is characterized by higher fission rate of peroxisome [46], the data points follow the trend of the theory curve, barring the data point representing the WT yeast (not shown).

In conclusion, the key finding of this section is that the *de novo* synthesis-fission-decay model, proposed by Mukherji

and O'Shea [23] and later built upon by Craven [25], cannot explain the single-cell peroxisome data, obtained from various different experimental studies.

V. MECHANISM OF ORGANELLE BIOGENESIS PREDICTS A BIMODAL DISTRIBUTION OF ORGANELLE ABUNDANCE

An idea that has gained much traction in recent years is the possibility of achieving phenotypic heterogeneity through nongenetic mechanisms [47]. A large number of studies have focused on how noise and bimodality in gene expression can lead to phenotypic diversification [27,47]. Interestingly, a recent commentary by Chang and Marshall [24] hints at the possible role of the cell-to-cell variability of organelles in leading to distinct phenotypes. In this light, we theoretically explore the following question: Can mechanisms of biogenesis drive bimodality in organelle abundance? In order to answer this query, we look into the full model consisting of all the four processes. We find that when the rate of *de novo* synthesis is much smaller than the fission rate, the model predicts a bimodal distribution of organelle abundance across a cell population, as shown in Fig. 3(b). As discussed earlier, cells increase the number of organelles through *de novo* synthesis and fission. Fission happens when there is at least a single organelle copy in the cell. When the number of an organelle in a cell goes to zero, the cell remains in this state until the organelle number becomes 1 through a *de novo* synthesis event. Once the number of the organelle goes to 1, the cell can start producing them through fission and the number can quickly increase. Hence, for when the rate of *de novo* synthesis is much smaller compared to the fission rate, the cells either remain in the zero-organelle state or produce a finite number of organelles, depending on the fusion and decay rate. It must be noted that the fusion and decay rates should be of comparable magnitude for bimodality to arise. While the fission rate should be higher than the rate of fusion and decay for the second mode of the distribution to exist, for when the fission rate is much greater than the fusion and decay rate, the first mode of the distribution corresponding to the zero-organelle state ceases to exist. It must be noted that none of the six limiting models manifest bimodality. It would be interesting to explore the case where abundance of any organelle exhibits bimodality.

VI. DISCUSSION

Cell-to-cell variability in organelle abundance in a population of cells can be exploited to unravel the governing principles of organelle biogenesis. While the strategy of using cell-to-cell variability to gain mechanistic insights has led to a number of crucial discoveries in different areas of molecular and cellular biology, such as gene expression [48,49] and flagellar rotation [50], it remains less utilized in understanding the regulation of organelle abundance, except for a few studies [2,23,51]. In this paper, we explore a general model [23] of organelle biogenesis and explore the relative contributions of different processes associated with this model in controlling the noise in organelle abundance. In order to achieve this goal, we compute the closed-form steady-state organelle number distributions for each of the limiting models of the general model and the corresponding means and variances. Using these analytical results, we show that the change in the Fano factor of an organelle number distribution as a function of the various parameters leads to distinct predictions for the different mechanisms of organelle biogenesis. These specific predictions of the organelle number distribution not only complement the traditional microscopy experiments but also provide a powerful quantitative lens to extract deeper mechanistic insights from them.

We elucidate the utility of our theory by applying it to published data for peroxisome abundance in *Saccharomyces cerevisiae* [38,52]. We show that the *de novo* synthesis-fission-decay model, proposed in recent studies [23,25], cannot explain single-cell peroxisome counts obtained from other experimental studies [39]. Rather, a general model consisting of all the four processes, namely, *de novo* synthesis, fission, decay, and fusion can capture the trend of the data. While experimental findings suggest that mature peroxisomes do not fuse in yeast, it remains debated [45,53]. It was suggested [45,53] that the possibility of peroxisome fusion under certain metabolic or environmental conditions cannot be excluded. In spite of the close match between the predictions of the *de novo* synthesis-fission-fusion-decay model, and peroxisome measurements, we cannot explicitly rule out other possible mechanisms of regulation of peroxisome abundance. For instance, an alternative possibility is that cells control the number of peroxisomes through some feedback mechanism [1]. It was shown in an experimental study [54] that HEX oligomers through a positive feedback mechanism provide a way of controlling composition and abundance of peroxisomes. Also, it has been shown that the rate of peroxisome decay via autophagy depends on the existence of a functional fission pathway [55]. It is possible to extend our model to incorporate some of these findings. For example, in the case of fission-dependent autophagy rates, the decay rate constant can be expressed as a function of the fission rate constants. More importantly, deviations from this simple model could actually pave the way for discovering the abovementioned mechanisms of organelle abundance control, such as the coupling between the different processes affecting organelle copy number, organelle-size-dependent rates or feedback [2], etc. Nonetheless, we make use of the *de novo* synthesis-fission-fusion-decay model as a simple scenario that explains the data and provides mechanistic insights into the process of peroxisome biogenesis that leads to experimentally testable predictions.

We apply our theory to peroxisome data to demonstrate the utility of our theory; nevertheless, our modeling framework is rather general in spite of its simplicity and is not limited to peroxisome. The processes this model incorporates have been experimentally observed in the context of biogenesis of various organelles such as vacuole, Golgi body, mitochondria, etc. [23,25].

One key question our paper deals with is whether cell-to-cell variability in organelle abundance plays any functional role [24]. While many studies to date have identified molecular-level variability such as gene expression noise as an important source of phenotypic heterogeneity [27,47], it is not clear if organelle-level heterogeneity can play a role, if any, in

creating phenotypic variability [24]. In a recent commentary, Chang and Marshall [24] hypothesized a possible role of cell-to-cell organelle variability in the context of disease, in particular, if some diseases exhibit more or less variability compared to nondiseased states [56]. Our analytical results concretize this hypothesis by making specific and experimentally testable predictions for generating bimodality in organelle abundance, where the two modes of the distribution can signify two different phenotypes. It must be noted that other scenarios where the various rate constants depend on organelle composition and size can also potentially lead to bimodality.

In conclusion, we have provided a theoretical framework and related analytical tools to analyze single-cell experiments that produce organelle number distribution, to extract information about the dynamics of organelle biogenesis in cells. The combination of single-cell experiments and theory holds the promise of uncovering comprehensive kinetic information about the process of organelle biogenesis.

VII. MATERIALS AND METHODS

A. On the conditions of reaching the stationary state

The general model as shown in Fig. 1(a) consists of four processes, namely, *de novo* synthesis, fission, fusion, and decay. While *de novo* synthesis and fission increase the number of organelles, fusion, and decay decrease their number, as shown in Fig. 1(b). Through an interplay between these opposing processes, the distribution of organelle abundance becomes stationary. Evidently, any possible combination of these processes should at the least consist of one process that increases organelle number and one process that decreases organelle number. We can in principle construct four limiting models that are combinations of two processes: *de novo* synthesis-decay, fission-fusion, *de novo* synthesis-fusion, fission-decay. However, out of these four combinations, the fission-decay model does not have any steady state. When the fission rate constant is much greater than the decay rate constant, the number of organelles tends to keep growing. On the other hand, when the rate constant of decay is greater than the fission rate constant, the organelle number eventually goes to zero. The cell remains in this state since for fission to increase the number of organelles the cell needs to have at least one organelle copy. Hence the fission-decay model does not lead to a steady state where the organelle number is finite.

For combinations of three processes, there are four possible limiting models: *de novo* synthesis-fission-fusion, *de novo* synthesis-fusion-decay, *de novo* synthesis-fission-decay, fission-fusion-decay. Amongst these limiting models, we note that the *de novo* synthesis-fission-decay process reaches a steady state only when the fission rate constant is lesser than the decay rate constant. Otherwise, the organelle number keeps growing. When the decay rate constant is greater than the fission rate constant, the organelle number does not get frozen at the zero-organelle state due to the presence of *de novo* synthesis. Thus, the inclusion of *de novo* synthesis to the fission-decay model leads to a nontrivial steady state. This same line of argument shows that a combination of fission, fusion, and decay cannot also reach a steady state in the absence of *de novo* synthesis. All other combinations of the processes, as mentioned above, naturally lead to steady-state conditions for any choice of the rates. Along the same lines, it can be argued that the fission-fusion-decay model does not have a nontrivial steady state.

In this paper, we consider those models which show stationarity in the strict mathematical sense. Let us consider the fission-decay model. For this model, once the system reaches the zero-organelle state it remains there forever. Hence in the limit of the decay rate constant being higher than the fission rate constant, there exists a trivial steady state. However, if the fission rate constant is much higher than the decay rate constant, the system may never go to the zero-organelle state. The same goes for the fission-fusion-decay model. Hence one cannot rule out the possibility of fission-decay or fission-fusion-decay model being biologically relevant if the rate constant of the fission process is much greater than the decay rate constant.

B. Detailed balance

Here we employ the detailed balance condition following Refs. [25,26] to obtain the steady-state organelle number distribution. To justify the applicability of the detailed balance condition, we follow the same line of argument as Ref. [57]. Let us consider two organelle number states, i and j. Moreover, let J_{ij} denote the steady-state probability current between two states i and j, given by $J_{i\to j} = P(i)W_{i\to j} - P(j)W_{j\to i}$, where $P(i)$ is the probability of having i number of organelles. Here $W_{i\to j}$ is the transition rate from the ith to the jth state. The state space for the organelle numbers does not have any loops because the numbers go linearly from 0, to 1, from 1 to 2, and so on. Correspondingly, the steady state is characterized by a single constant probability current J. Furthermore, because $P(N)$ tends to zero for large N, we must have $J = 0$. Thus, all probability currents vanish in the steady state. Hence, at the steady state, the detailed balance condition would imply that the frequency of transition from a state of n organelle copies to the state of $n-1$ organelle copies must equal the frequency of transition from $n-1$ organelle copy state to n organelle copy state, where $n = \{0, 1, 2, \ldots\}$. For instance, if we consider the *de novo* synthesis-decay model, the detailed balance condition would imply the following mathematical condition:

$$k_d P(n-1) = \gamma n P(n).$$

Here the probability of having $n-1$ and n organelles in the cell is given by $P(n-1)$ and $P(n)$, respectively. The rate of *de novo* synthesis is given by k_d, and γ is rate of decay. This recursion relation allows us to find a relationship between the probability of having n organelles $P(n)$, and zero organelles $P(0)$ in the cell, respectively, which is given by

$$P(n) = \frac{1}{n!}\left(\frac{k_d}{\gamma}\right)^n P(0).$$

It is evident that $P(0)$ has to be evaluated for obtaining the exact expression for $P(n)$. To achieve this goal, we use the

normalization condition that

$$\sum_{n=0}^{\infty} P_n = 1,$$

$$\sum_{n=0}^{\infty} \frac{1}{n!}\left(\frac{k_d}{\gamma}\right)^n P(0) = 1.$$

We can evaluate this sum using MATHEMATICA and get a final expression for $P(n)$, which is given by

$$P(n) = \frac{1}{n!}\left(\frac{k_d}{\gamma}\right)^n \exp\left(-\frac{k_d}{\gamma}\right).$$

Similarly, the distribution of organelle abundance for all the different limits of the general model as well the full model can be obtained. Using standard functions in MATHEMATICA, we can also obtain the mean and variance of the organelle distribution for all the models. We have also attached a MATHEMATICA file as a Supplemental Material [38,58].

C. Limitations of the model

The model of organelle biogenesis we explore here is an "effective" model, where we assume the different rates to be constant. It is potentially a simplistic assumption as some of these rates can depend on the size of the organelles i as the fusion rate of peroxisomes [59]. While it is possible to incorporate such size dependence, we believe that the model considered here provides the simplest scenario and hence provides the null predictions. Any deviation from these models would hint at the presence of other more complicated mechanisms such as organelle-size-dependent rates or feedback [2]. Two of the limiting models we consider in our analysis, (iii) *de novo* synthesis-fusion and (vi) *de novo* synthesis-fission-fusion models, do have steady states in terms of organelle number, but the mass of organelles would keep increasing indefinitely. Clearly, these models can be biologically relevant only if there are other cellular mechanisms such as possible membrane removal, etc. [21] to maintain mass balance without altering the organelle number. While we analyze these models for the sake of completeness, the obvious next step would be to consider size-dependent rates to explore how the model predictions change. This would allow us to also garner a clear understanding of how cells regulate the number and composition of organelles [1].

Some of the models we consider do not include decay, and the reduction in number of organelles happens through fusion. One would imagine that in cells, organelles would encounter some form of decay on account of the various cellular processes. However, if the decay rate constant is much smaller than the rate constant of fusion, then organelle abundance will still be primarily dictated by fusion.

D. Parameter extraction

We evaluate the utility of our analytical results by applying them to published data to gain mechanistic insights into the biogenesis of peroxisome. To this end, we have reanalyzed peroxisome single-cell count data. We extract the peroxisome data from the published peroxisome number distribution plots in Figs. 1(A)–1(J) of Ref. [39] by using DIGITIZEIT, a free online tool for digitizing data plots. From this distribution we compute the mean and Fano factor for the various mutant strains, as shown in Fig. 3(a).

Next, in order to make the Fano factor-mean prediction plot for *de novo* synthesis-fission-fusion-decay model [see blue curve in Fig. 3(a)], we fit the data for the dnm1-vps1 double-deletion yeast strain with the *de novo* synthesis-fusion-decay model to find the values of the individual rates. Here we assume that the fission rate for this strain is vanishing since two of the known fission factors are not present in the cells. It must be noted that we cannot uniquely determine the kinetic rate constants associated with the different processes defining the *de novo* synthesis-fusion-decay model since the distribution of organelle abundance corresponding to different mechanisms depends on the ratios of the parameters. Hence, we need to set the value of one of the rate constants to 1 and measure the other rate constants with respect to that parameter. The value of the decay rate constant is set to 1. We extract the following parameters: $k_{\rm fus} = 36.39\,t^{-1}$, $k_d = 3.46\,t^{-1}$, and $\gamma = 1\,t^{-1}$, $k_{\rm fis} = 0\,t^{-1}$.

Error bars in Fano factor [Fig. 3(a)] represent the standard deviation of 1000 independent, resampled data sets obtained using the method of Bootstrapping in MATLAB.

ACKNOWLEDGMENTS

We wish to thank Tylor Herman and Sakunatala Chatterjee for detailed comments on the manuscript. S.C. would like to thank Shankar Mukherji for his initial inputs.

[1] W. F. Marshall, Cell geometry: How cells count and measure size, Annu. Rev. Biophys. **45**, 49 (2016).

[2] W. F. Marshall, Stability and robustness of an organelle number control system: Modeling and measuring homeostatic regulation of centriole abundance, Biophys. J. **93**, 1818 (2007).

[3] M. Yan, N. Rayapuram, and S. Subramani, The control of peroxisome number and size during division and proliferation, Curr. Opin. Cell Biol. **17**, 376 (2005).

[4] K. L. Cerveny, Y. Tamura, Z. Zhang, R. E. Jensen, and H. Sesaki, Regulation of mitochondrial fusion and division, Trends Cell Biol. **17**, 563 (2007).

[5] Y. Desfougères, Organelle size control: Accumulating vacuole content activates SNAREs to augment organelle volume by homotypic fusion, J. Cell Sci. **43**, 2817 (2016).

[6] G. Agrawal and S. Subramani, De novo peroxisome biogenesis: Evolving concepts and conundrums, Biochim. Biophys. Acta **1863**, 892 (2016).

[7] L. Dimitrov, S. K. Lam, and R. Schekman, The role of the endoplasmic reticulum in peroxisome biogenesis, Cold Spring Harbor Perspect. Biol. **5**, a013243 (2013).

[8] M. Lowe and F. A. Barr, Inheritance and biogenesis of organelles in the secretory pathway, Nat. Rev. Mol. Cell. Biol. **8**, 429 (2007).

[9] K. W. Osteryoung, Organelle fission in eukaryotes, Curr. Opin. Microbiol. **4**, 639 (2001).

[10] L. Hofmann, R. Saunier, R. Cossard, M. Esposito, T. Rinaldi, and A. Delahodde, A nonproteolytic proteasome activity controls organelle fission in yeast, J. Cell Sci. **122**, 3673 (2009).

[11] B. Westermann, Organelle dynamics: ER embraces mitochondria for fission, Curr. Biol. **21**, R922 (2011).

[12] C. Denesvre and V. Malhotra, Membrane fusion in organelle biogenesis, Curr. Opin. Cell. Biol. **8**, 519 (1996).

[13] M. Verhage, Organelle docking: R-SNAREs are late, Proc. Natl. Acad. Soc. USA **106**, 19745 (2009).

[14] Y. Desfougères, S. Vavassori, M. Rompf, R. Gerasimaite, and A. Mayer, Organelle acidification negatively regulates vacuole membrane fusion *in vivo*, Sci. Rep. **6**, 29045 (2016).

[15] W. Wickner and A. Haas, Yeast homotypic vacuole fusion: A window on organelle trafficking mechanisms, Annu. Rev. Biochem. **69**, 247 (2000).

[16] O. Müller, D. I. Johnson, and A. Mayer, Cdc42p functions at the docking stage of yeast vacuole membrane fusion, EMBO J. **20**, 5657 (2001).

[17] J. P. Luzio, Y. Hackmann, N. M. G. Dieckmann, and G. M. Griffiths, The biogenesis of lysosomes and lysosome-related organelles, Cold Spring Harbor Perspect. Biol. **6**, a016840 (2014).

[18] P. Saftig and J. Klumperman, Lysosome biogenesis and lysosomal membrane proteins: Trafficking meets function, Nat. Rev. Mol. Cell. Biol. **10**, 623 (2009).

[19] A. van der Vaart, M. Mari, and F. Reggiori, A picky eater: Exploring the mechanisms of selective autophagy in human pathologies, Traffic **9**, 281 (2008).

[20] A. R. Kristensen, S. Schandorff, M. Høyer-Hansen, M. O. Nielsen, M. Jäättelä, J. Dengjel, and J. S. Andersen, Ordered organelle degradation during starvation-induced autophagy, Mol. Cell. Proteomics **7**, 2419 (2008).

[21] A. L. Anding and E. H. Baehrecke, Cleaning house: Selective autophagy of organelles, Dev. Cell. **41**, 10 (2017).

[22] A. M. van der Bliek, Q. Shen, and S. Kawajiri, Mechanisms of mitochondrial fission and fusion, Cold Spring Harbor Perspect. Biol. **5**, a011072 (2013).

[23] S. Mukherji and E. K. O'Shea, Mechanisms of organelle biogenesis govern stochastic fluctuations in organelle abundance, eLife **3**, e02678 (2014).

[24] A. Y. Chang and W. F. Marshall, Organelles – understanding noise and heterogeneity in cell biology at an intermediate scale, J. Cell Sci. **130**, 819 (2017).

[25] C. J. Craven, Evaluation of predictions of the stochastic model of organelle production based on exact distributions, eLife **5**, e10167 (2016).

[26] N. G. V. Kampen, *Stochastic Processes in Physics and Chemistry*, 3rd ed. (North Holland, Amsterdam, 2007).

[27] A. Sanchez, S. Choubey, and J. Kondev, Regulation of noise in gene expression, Annu. Rev. Biophys. **42**, 469 (2013).

[28] B. J. Bevis, A. T. Hammond, C. A. Reinke, and B. S. Glick, *De novo* formation of transitional ER sites and Golgi structures in *Pichia pastoris*, Nat. Cell Biol. **4**, 750 (2002).

[29] O. W. Rossanese, J. Soderholm, B. J. Bevis, I. B. Sears, J. O'Connor, E. K. Williamson, and B. S. Glick, Golgi structure correlates with transitional endoplasmic reticulum organization in Pichia pastoris and Saccharomyces cerevisiae, J. Cell Biol. **145**, 69 (1999).

[30] E. Losev, C. A. Reinke, J. Jellen, D. E. Strongin, B. J. Bevis, and B. S. Glick, Golgi maturation visualized in living yeast, Nature (London) **441**, 1002 (2006).

[31] K. Matsuura-Tokita, M. Takeuchi, A. Ichihara, K. Mikuriya, and A. Nakano, Live imaging of yeast Golgi cisternal maturation, Nature (London) **441**, 1007 (2006).

[32] S. Michaeli and G. Galili, Degradation of organelles or specific organelle components via selective autophagy in plant cells, Int. J. Mol. Sci. **15**, 7624 (2014).

[33] *Handbook of Mathematical Functions: with Formulas, Graphs, and Mathematical Tables*, edited by M. Abramowitz and I. A. Stegun, 0009-Revised ed. (Dover, New York, 1965).

[34] G. Andrews, R. Askey, and R. Roy, *Special Functions*, 1st ed. (Cambridge University Press, Cambridge, 2001).

[35] I. Scott and R. J. Youle, Mitochondrial fission and fusion, Essays Biochem. **47**, 85 (2010).

[36] R. J. Youle and A. M. van der Bliek, Mitochondrial fission, fusion, and stress, Science **337**, 1062 (2012).

[37] Z. Y. Tam, J. Gruber, B. Halliwell, and R. Gunawan, Mathematical modeling of the role of mitochondrial fusion and fission in mitochondrial DNA maintenance, PLoS ONE **8**, e76230 (2013).

[38] See Supplemental Material at http://link.aps.org/supplemental/10.1103/PhysRevE.100.022405 for additional figures and a MATHEMATICA file.

[39] K. Kuravi, S. Nagotu, A. M. Krikken, K. Sjollema, M. Deckers, R. Erdmann, M. Veenhuis, and I. J. van der Klei, Dynamin-related proteins Vps1p and Dnm1p control peroxisome abundance in Saccharomyces cerevisiae, J. Cell Sci. **119**, 3994 (2006).

[40] E. H. Hettema, R. Erdmann, I. van der Klei, and M. Veenhuis, Evolving models for peroxisome biogenesis, Curr. Opin. Cell Biol. **29**, 25 (2014).

[41] P. Kim, Peroxisome biogenesis: A union between two organelles, Curr. Biol. **27**, R271 (2017).

[42] D. Hoepfner, D. Schildknegt, I. Braakman, P. Philippsen, and H. F. Tabak, Contribution of the endoplasmic reticulum to peroxisome formation, Cell **122**, 85 (2005).

[43] A. Huber, J. Koch, F. Kragler, C. Brocard, and A. Hartig, A subtle interplay between three Pex11 proteins shapes de novo formation and fission of peroxisomes, Traffic **13**, 157 (2012).

[44] Ł. Opaliński, J. A. K. W. Kiel, C. Williams, M. Veenhuis, and I. J. van der Klei, Membrane curvature during peroxisome fission requires Pex11, EMBO J. **30**, 5 (2011).

[45] M. Schrader, N. A. Bonekamp, and M. Islinger, Fission and proliferation of peroxisomes, Biochim. Biophys. Acta, Mol. Basis Dis. **1822**, 1343 (2012).

[46] R. Saraya, M. Veenhuis, and I. J. van der Klei, Peroxisomes as dynamic organelles: peroxisome abundance in yeast, FEBS J. **277**, 3279 (2010).

[47] J. M. Raser and E. K. O'Shea, Noise in gene expression: Origins, consequences, and control, Science **309**, 2010 (2005).

[48] B. Munsky, G. Neuert, and A. van Oudenaarden, Using gene expression noise to understand gene regulation, Science **336**, 183 (2012).

[49] A. Sanchez, S. Choubey, and J. Kondev, Stochastic models of transcription: From single molecules to single cells, Methods **62**, 13 (2013).

[50] A. D. Samuel and H. C. Berg, Fluctuation analysis of rotational speeds of the bacterial flagellar motor, Proc. Natl. Acad. Sci. USA **92**, 3502 (1995).

[51] A. S. Hennis and C. W. Birky, Stochastic partitioning of chloroplasts at cell division in the alga Olisthodiscus, and compensating control of chloroplast replication, J. Cell Sci. **70**, 1 (1984).

[52] I. Yofe, K. Soliman, S. G. Chuartzman, B. Morgan, U. Weill, E. Yifrach, T. P. Dick, S. J. Cooper, C. S. Ejsing, M. Schuldiner *et al.*, Pex35 is a regulator of peroxisome abundance, J. Cell Sci. **130**, 791 (2017).

[53] N. Shai, M. Schuldiner, and E. Zalckvar, No peroxisome is an island — Peroxisome contact sites, Biochim. Biophys. Acta **1863**, 1061 (2016).

[54] F. Liu, Y. Lu, L. Pieuchot, T. Dhavale, and G. Jedd, Import oligomers induce positive feedback to promote peroxisome differentiation and control organelle abundance, Dev. Cell. **21**, 457 (2011).

[55] K. Mao, X. Liu, Y. Feng, and D. J. Klionsky, The progression of peroxisomal degradation through autophagy requires peroxisomal division, Autophagy **10**, 652 (2014).

[56] M. P. Jogalekar and E. E. Serrano, Morphometric analysis of a triple negative breast cancer cell line in hydrogel and monolayer culture environments, Peer J. **6**, e4340 (2018).

[57] N. Kumar, K. Zarringhalam, and R. V. Kulkarni, Stochastic modeling of gene regulation by noncoding small RNAs in the strong interaction limit, Biophys. J. **114**, 2530 (2018).

[58] The MATHEMATICA file can also be found on Github: https://github.com/schoubey123/Analytical_Calculations.

[59] M. Schrader and H. D. Fahimi, Growth and division of peroxisomes, Int. Rev. Cytol. **255**, 237 (2006).